JOURNAL OF MATERIALS SCIENCE **39** (2004) 3369– 3373

Investigation of elastic modulus of nanoporous alumina membrane

P. GU*, H. MIAO, Z. T. LIU, X. P. WU, J. H. ZHAO
Department of Mechanics and Mechanical Engineering, University of Science and Technology of China, Key Laboratory of Material Mechanical Behavior and Design of Chinese Academy of Science, Hefei 230027, People's Republic of China
E-mail: guping@ustc.edu.cn

Nanoporous alumina membranes containing parallel regular pores of uniform size and normal to substrate surface were fabricated by anodically oxidizing high purity aluminum foils in acid solutions and their elastic modulus was investigated. The continuous out-of-plane displacement and current load of the porous membranes were obtained through bulge test combining real-time ESPI (electronic speckle pattern interferometry) observation system. Then the elastic modulus was calculated through an analytical model and the pore distortion after load was characterized by HRSEM (high resolution scan electron microscope). Measurement of mechanical properties indicates unusual mechanical behavior of these anodic alumina films compared with bulk alumina materials. This observation may help shed light on fracture mechanism of these films with nanopore arrays and bring further understanding on connecting of micro-meso structure and mechanical properties.

1. Introduction

The AAO (anodic aluminum oxide) membrane, which is achieved by an anodic oxidation of aluminum in appropriate electrolyte solutions and anodizing voltages, is a typical self-ordered nanoporous materials [1, 2]. The AAO membrane has a packed array of columnar hexagonal cells with central, cylindrical, uniform size holes ranging from 4 to 200 nm in diameter. There has been increasing interest in anodic alumina membrane due to its unique structure and self-organization, as well as potentially wide applications in filtering and separating membrane [3, 4]. Furthermore, it provides a convenient route for fabricating 1D nanostructures with various size and shape by using alumina membranes as templates [5, 6]. However, their mechanical properties have been scarcely reported. In this paper, the continuous out-of-plane displacement and current load of the porous films were obtained through bulge test combining real-time ESPI (electronic speckle pattern interferometry) observation system and the elastic modulus of the porous alumina membranes was calculated through an analytical model. The pore distortion was characterized by HRSEM (high resolution scan electron microscope). This observation may help shed light on application of these membranes with nanopore arrays and bring further understanding on connecting of micro-meso structure and mechanical properties.

2. Experimental procedures

In our experiment, the ordered AAO membrane was prepared by a two-step anodization [7]. In brief, ultra-pure Al (99.999%) sheet was degreased, annealed and electrochemical polished. Then the Al sheet was anodized for the first time in a 0.3 M oxalic acid solution at 14°C under constant voltage of 40 V for 8 h.The formed porous alumina membrane was removed by a wet chemical etching in a mixture of phosphoric acid (6 wt%) and chromic acid (1.8 wt%) at 60°C for 5 h. Subsequently, the Al sample was anodized again for 8 h under identical conditions to those of the first anodization. Then the remaining Al substrate and the barrier layer on the bottom side of the sample were removed by using a 0.3 M $SnCl_4$ solution and a 6 wt% phosphoric acid solution respectively at 30°C for 30 min. The obtained alumina membrane was characterized by scanning electron microscopy (SEM, Jeol JSM-6300) and transmission electron microscopy (TEM, JEM-200CX) in Fig. 1.

Fig. 1a shows the SEM image of the surface and Fig. 1b shows cross-section view of the AAO membrane. It can be clearly seen that an excellent close-packed array of approximately hexagonal cells is formed in this case. The average pore diameters and pore lengths are 50 nm and 76 μm respectively. The sample was sealed by O-ring and epoxy on a stainless steel plate center where is a 10-millimeter diameter hole and then pressed evenly by a slack airpocket in

*Author to whom all correspondence should be addressed.

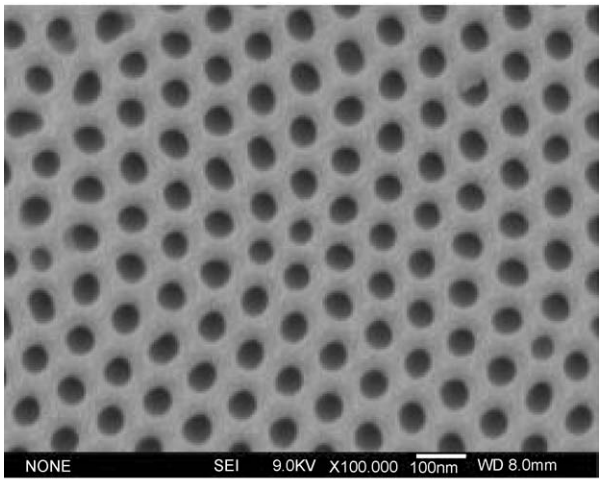

a

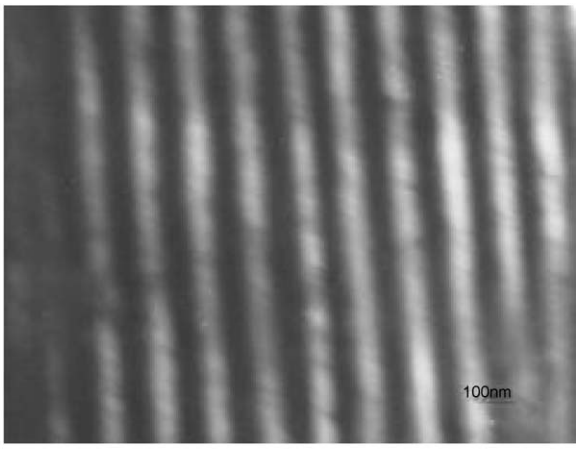

b

Figure 1 Images of the anodic alumina membrane: (a) SEM image of the top surface, (b) TEM image of the cross-section view.

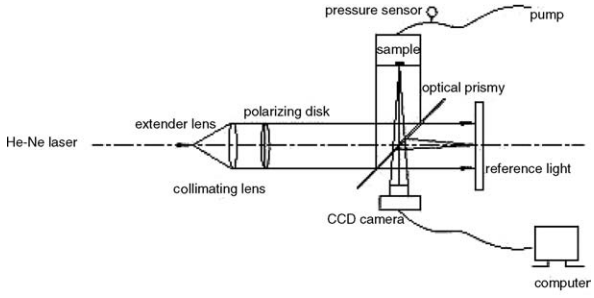

(a)

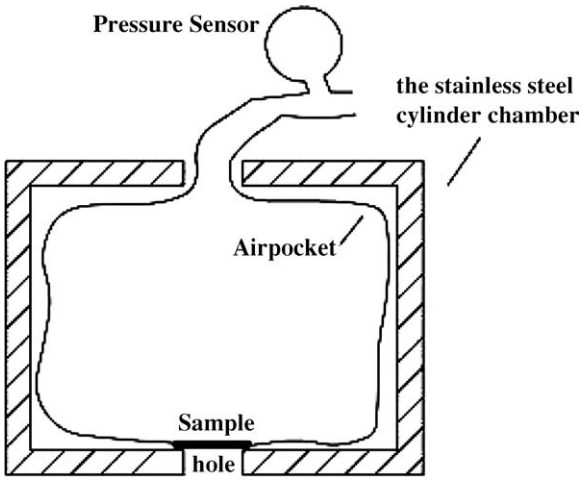

(b)

Figure 2 (a) Schematic diagram of apparatus for bulge test combining real-time ESPI observation system. (b) Schematic diagram of the bulging adapter.

the stainless steel cylinder adapter, as shown in Fig. 2b, then fixed in light path.

The mechanical property of alumina membrane was tested by bulge technique, which was proposed by Beams [8]. In our experiment, bulge test combining real-time ESPI observation system is consisted of four parts: ESPI optical setup, bulging adapter, real-time observation and image acquisition system, and air pressure control equipment, seen in Fig. 2a. ESPI optical setup is a typical Michelson interferometry set on an optical platform with vibration isolators. Bulging adapter is the combination of steel cylinder, sample and airpocket. Air pressure control is fulfilled by using an electric air pump, pneumatic cushion chamber, valves, airpocket and pressure sensor. Real-time observation and image acquisition system is composed of an image acquisition board, a CCD camera and a computer. Pressure was applied to the membrane by introducing air through the opening in the airpocket. While pressure was continuously monitored by adjusting the valves, the membrane began to deform and form bulge. The load acted on the membrane could be calculated directly from the difference between air pressure in airpocket and atmospheric pressure. Through pressure sensor and real-time ESPI observation system, a series of current loads and corresponding ESPI images, which include out-of-plane displacements information, were recorded. After mean filtering treatment, grey level map of recorded fringes was obtained and the order of fringes in membrane can be known. According to our optical setup, one fringe represents $\lambda/2$ out-of-plane displacement, in which λ is 0.6328 μm, the wavelength of He-Ne laser. After the continuous out-of-plane displacement and current load of the porous films were obtained, the elastic modulus of the porous alumina films was calculated through an analytical model of low flexibility deformation of circular clamped disk by uniform pressure.

3. Results and discussion

A series of ESPI images obtained by bulge testing and their corresponding fringes images and grey level maps were obtained. Some of them are shown in Fig. 3. Since the initial state of the alumina membrane was not smooth and experimental data obtained under elastic deformation is useful, pressure applied on membrane was slightly higher than air pressure and experimental data were recorded after the deformation became regular. Fig. 3A(a), 3B(a) and 3C(a) are ESPI images obtained by adjusting bulging pressure from 101.40 to 101.55 KPa, 101.55 to 101.70 KPa and 101.70 to 101.85 KPa, respectively. Fig. 3A(b) and 3A(c) are fringe images after mean filtering and grey level distribution of the line in 3A(b). From Fig. 3A(c), the order number of black stripe in 3A(a) can be deduced as 3.5.

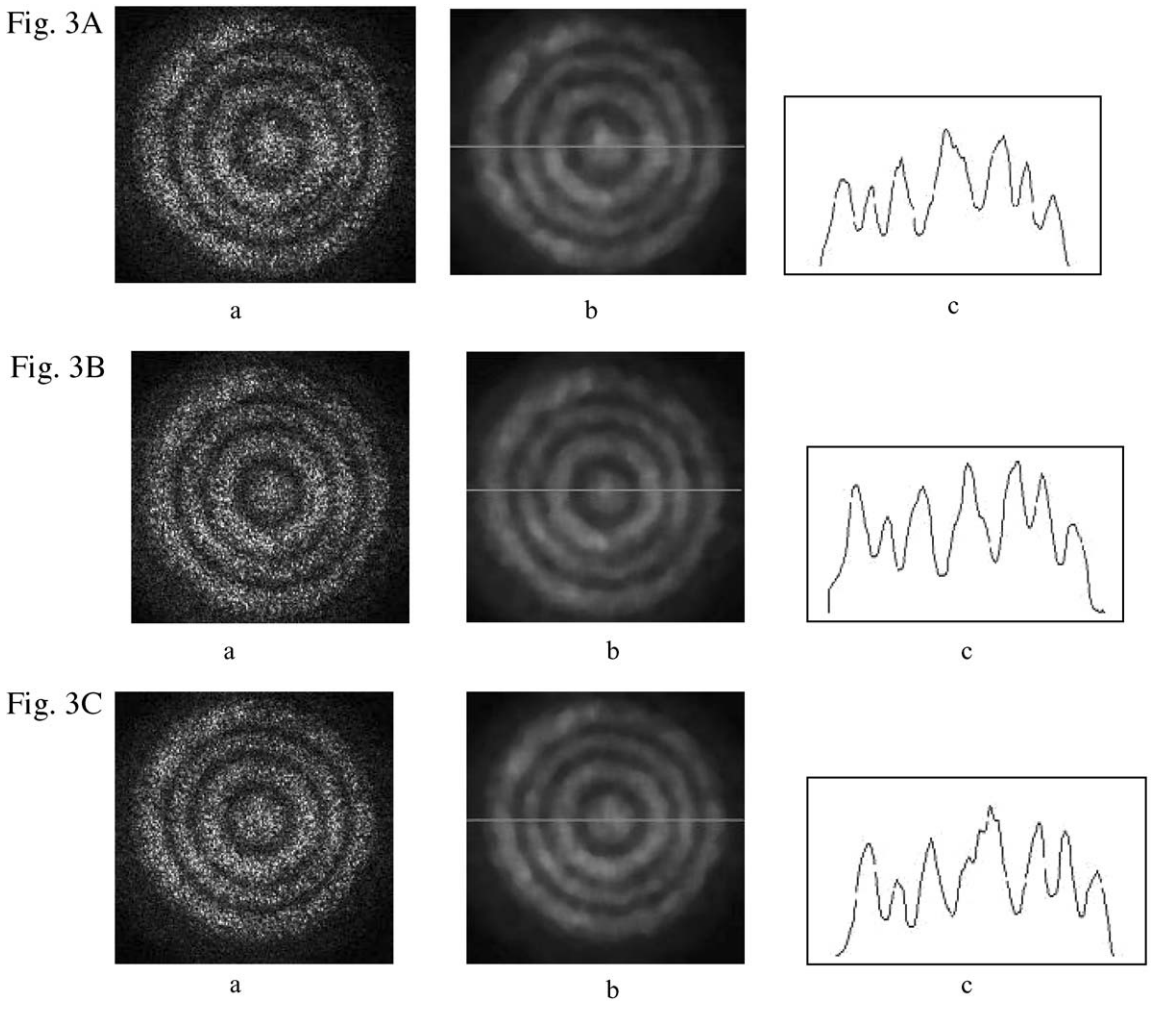

Figure 3 Experimental data obtained by adjusting bulging pressure from (A) 101.40 to 101.55 KPa, (B) 101.55 to 101.70 KPa, (C) 101.70 to 101.85 KPa. (a) ESPI image, (b) stripe image after wave filtering, and (c) grey-scale distribution of the line in b.

Similarly, the order numbers of black fringe Fig. 3B(a) and Fig. 3C(a) also equal to 3.5, which means under a load adding of 0.15 KPa, the out-of-plane displacement increment of sample center is 1.1074 μm, calculated by 3.5 $\times$ (λ/2) μm. Furthermore, the load increment and the out-of-plane displacement increment of sample center take on good linearity in experiment scope, as seen in Fig. 4, so the elastic modulus of the porous alumina films can be calculated through the formulation of low flexibility deformation of circular clamped disk under homogeneous load.

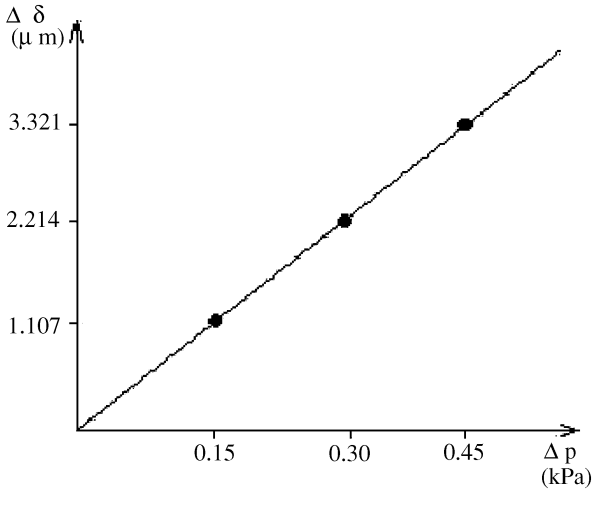

Figure 4 The dependence of out-of-plane displacement increment on load increment for nanoporous alumna membrane.

The relationship between load, out-plane displacement and elastic modulus is given by

$$W(r) = \frac{q(a^2 - r^2)^2}{64D} \tag{1}$$

$$D = \frac{Eh^3}{12(1 - \upsilon^2)} \tag{2}$$

$$\frac{\partial w}{\partial q} = \frac{12(a^2 - r^2)^2(1 - \upsilon^2)}{64Eh^3} \tag{3}$$

where $w(r)$ is the out-of-plane displacement of membrane, r and a are radius coordinate and radius of the hole respectively, also h is the membrane thickness, q is load, υ is Passion ratio (approximately 0.32) and D is stiffness. The connection of Δq and $\Delta w(r)$ can be obtained by differentiating these two equations above, seen in Equation 3. When Δq is 150 Pa and r is 0 μm, Δw is 1.1074 μm, E is deduced as 32.5 GPa through Equation 3. The SEM images of the surface and cross-section view of the AAO membrane after bulging test are shown in Fig. 5. There are no obvious changes on pore diameter and distribution from

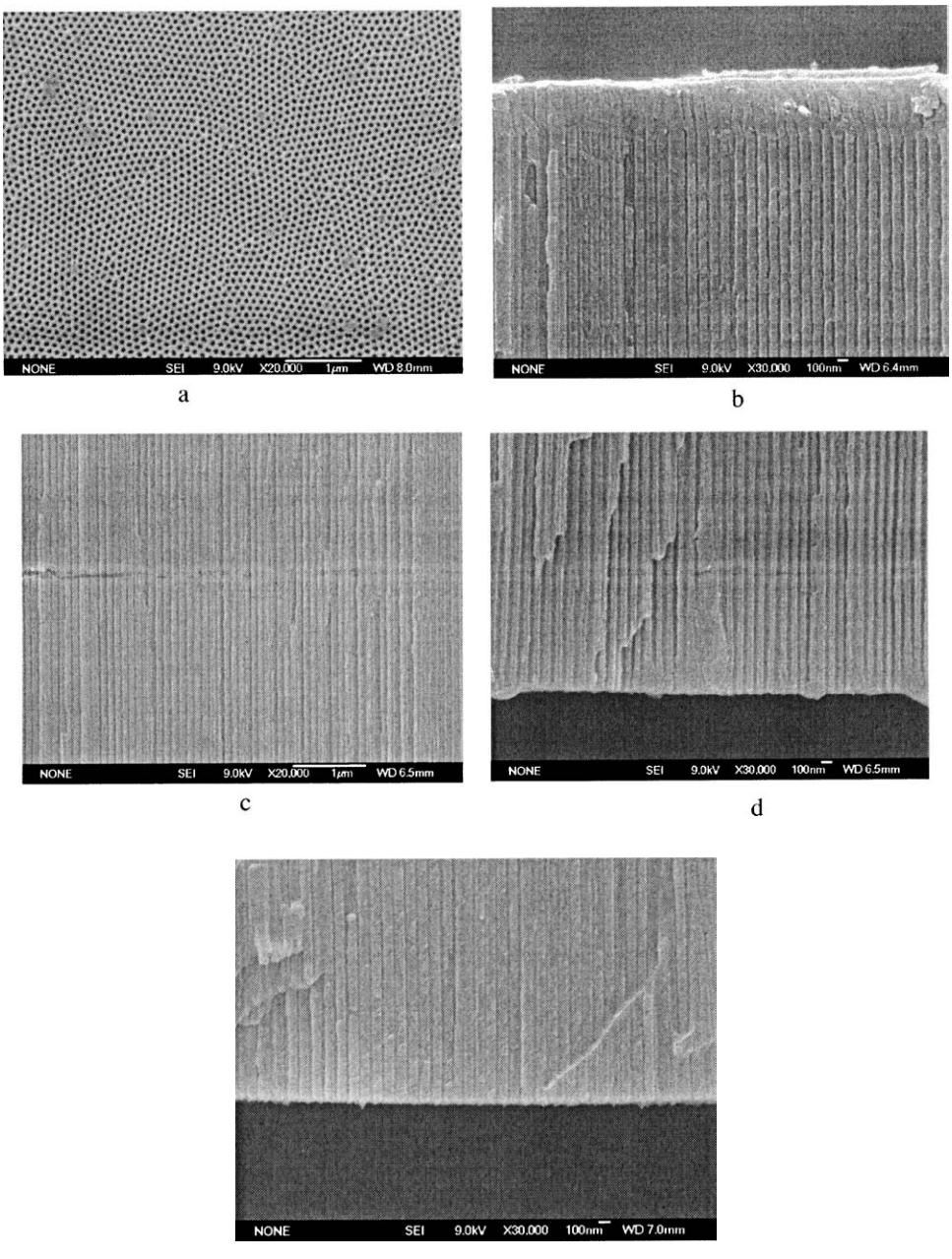

Figure 5 SEM images of the surface and cross-section view of the AAO membrane after bulging test: (a) the surface, (b) nanopore array on the end of tension face, (c) nanopore array in the middle of the membrane, and (d) nanopore array on the other end. (e) SEM image of the cross-section view of the fresh membrane before the bulge test.

Fig. 5a, and the nanopore array keeps straight except one tilted layer near the tension face of the membrane, as seen in Fig. 5b, c, and d. Fig. 5e is the SEM image of the cross-section view of the fresh membrane before the bulge test. The elastic modulus is smaller than the value for bulk alumina ceramics (380–400 GPa for hot-pressed Al_2O_3 ceramics [9]). The deformation mode is also different to bulk alumina, maybe induced by the difference on crystal phase and mesostructure. These nanoporous AAO membranes are mostly consisted of amorphous aluminum oxides [10], whereas dense alumina ceramics are often composed of α-Al_2O_3 crystals and showing the transgranular fracture mode [11].

But in fact, nanoporous alumina membrane is different from thin plate or thin film, the macro elastic modulus of alumina membrane is not so accurate by using any present model. Some new models or combining model should be sought for applying in this kind of membrane. Combining real-time ESPI observation system, the accuracy of displacement is improved greatly. So our result can be used as a reference and brings a convenient method to test mechanical properties of similar structures. But a further detailed investigation on mesostucture and mechanical properties should be examined.

4. Conclusions

The macro elastic modulus of nanoporous alumina membrane is obtained by using bulge testing combining real-time ESPI observation system. This observation brings a convenient and precise method to test the deformation of the membranes and to obtain mechanical

properties of similar structures. The mechanical properties can be used as reference in application of these membranes.

Acknowledgment

This work was supported by National Nature Science Foundation of China (10302026).

References

1. F. KELLER, M. S. HUNTER and D. L. ROBINSON, *J. Electrochem. Soc*. **100** (1953) 411.
2. G. E. THOMPSON, R. C. FURNEAUX, G. C. WOOD, J. A. RICHARDSON and J. S. GODE, *Nature* **272** (1978) 433.
3. KINGO ITAYA, *Jpn. J. Chem. Engr.* 17 (1984) 514.
4. AHMAD T. SHAWAQFEH and RUTH E. BALTUS, *J. Memb. Sci.* **157** (1999) 147.
5. C. A. HUBER, T. E. HUBER, M. SADOQI, J. A. LUBIN *et al., Science* **263** (1994) 800.
6. W. C. HU, D. W. GONG *et al.*, *Appl. Phys. Lett.* **79** (2001) 3080.
7. H. MASUDA and M. SATOH, *Jpn. J. Appl. Phys.* **35** (1996) L126.
8. J. W. BEAMS, C. A. NEUGEBAUER, J. D. NEWKIRK and J. D. VERMILYEA (eds.), in "The Structure and Properties of Thin Film" (Wiley, New York, 1959) p. 183.
9. WILLIAM D. CALLISTER, in "Materials Science and Engineering—An Introduction," 3rd ed. (Wiley, New York, 1994) p. 767.
10. Y. C. SUI, B. Z. CUI, L. MARTINEZ, R. PEREZ and D. J. SELLMYER, *Thin Solid Films* **406** (2002) 64.
11. L. GAO, H. Z. WANG and J. S. HONG *et al. J. Europ. Ceram. Soc.* **19** (1999) 609.
12. A. J. GRIFFIN, JR., F. R. BROTZEN and C. F. DUNN, *Thin Solid Films* **220** (1992) 265.

Received 7 May 2003
and accepted 28 January 2004